Adaptation mechanisms of Clostridioides difficile to auranofin and its impact on human gut microbiota

Cyril Anjou, Marie Royer, Émilie Bertrand, Marius Bredon, Julie Le Bris, Iria Alonso Salgueiro, Léo Caulat, Bruno Dupuy, Frédéric Barbut, Claire Morvan, et al.

npj | biofilms and microbiomes

Article

Published in partnership with Nanyang Technological University

https://doi.org/10.1038/s41522-024-00551-3

Adaptation mechanisms of *Clostridioides difficile* to auranofin and its impact on human gut microbiota

Cyril Anjou[1], Marie Royer[1,9,10], Émilie Bertrand[1,10], Marius Bredon[2,3,10], Julie Le Bris[4,5], Iria Alonso Salgueiro[2,3], Léo C. Caulat[1], Bruno Dupuy[1], Frédéric Barbut[6,7], Claire Morvan[1], Nathalie Rolhion[2,3] & Isabelle Martin-Verstraete[1,8]

Auranofin (AF), a former rheumatoid polyarthritis treatment, gained renewed interest for its use as an antimicrobial. AF is an inhibitor of thioredoxin reductase (TrxB), a thiol and protein repair enzyme, with an antibacterial activity against several bacteria including *C. difficile*, an enteropathogen causing post-antibiotic diarrhea. Several studies demonstrated the effect of AF on *C. difficile* physiology, but the crucial questions of resistance mechanisms and impact on microbiota remain unaddressed. We explored potential resistance mechanisms by studying the impact of TrxB multiplicity and by generating and characterizing adaptive mutations. We showed that if mutants inactivated for *trxB* genes have a lower MIC of AF, the number of TrxBs naturally present in clinical strains does not impact the MIC. All stable mutations isolated after AF long-term exposure were in the anti-sigma factor of σ^B and strongly affect physiology. Finally, we showed that AF has less impact on human gut microbiota than vancomycin.

Clostridioides difficile is a Gram-positive, anaerobic and spore-forming bacterium responsible for post-antibiotic gastrointestinal infections[1]. During dysbiosis, a switch of microbiota leading to a change of metabolites is observed favoring *C. difficile* colonization and infection[2,3]. Clinical signs of *C. difficile* infections (CDIs) are diarrhea, pseudo-membranous colitis and toxic megacolon, which can lead to the death of the patient[2]. Historically identified as a healthcare-associated infection, changes in epidemiology have been observed during the last years, with now around 25% of community-associated CDIs[4]. The symptoms of CDIs are caused by the toxins of *C. difficile*[5]. TcdA and TcdB cause disruption of the epithelial intestinal barrier[6,7], resulting in a strong inflammation with recruitment of immune cells and production of reactive oxygen and nitrogen species[6,8,9]. CDT is an additional binary toxin, only present in some strains, that is associated to severe infections and increased risk of recurrences[10,11]. Indeed, after a first episode, a high rate of recurrences (20–25%) is usually observed[12]. Risk factors of recurrences are age and the antibiotic treatment used[13]. Indeed, the use of large spectrum antibiotic treatment inducing a strong disruption of the gut microbiota favors recurrences while the gut microbiota recovery protects from recurrence. On the bacterial side, these recurrences are at least partly due to the production of spores, which allows dissemination and transmission of this anaerobe pathogen[5]. These spores are highly resistant to air and disinfectants, and are responsible for widespread contamination in hospital and for re-infection of patients[1]. Biofilms might be another mechanism of recurrences of CDI, favoring persistence in the gut during antibiotic treatment[14,15].

First-line antibiotics for CDIs are vancomycin (Van) and fidaxomicin (Fdx) as metronidazole (Mtz) is now recommended only for pediatric infections[16]. After one or more recurrences, alternative treatments are recommended such as addition to the antibiotic treatment of bezlotoxumab, an anti-TcdB monoclonal antibody, or fecal microbiota transplantation (FMT)[16]. The choice of therapy will depend on the severity of infection, the risk and number of recurrences and the cost of the treatment. Despite all these treatments, CDIs remain a challenge to treat. Around 200,000 and 500,000 cases a year are observed in Europe[17] and in the US[18], respectively,

[1]Institut Pasteur, Université Paris Cité, UMR CNRS 6047, Laboratoire Pathogenèse des Bactéries Anaérobies, F-75015 Paris, France. [2]Sorbonne Université, INSERM, Centre de Recherche Saint-Antoine, CRSA, Paris, France. [3]Paris Center for Microbiome Medicine (PaCeMM) FHU, Paris, France. [4]Microbial Evolutionary Genomics, Institut Pasteur, CNRS UMR3525, Université Paris Cité, Paris, France. [5]Sorbonne Université, Collège Doctoral, École Doctorale Complexité du Vivant, 75005 Paris, France. [6]Université Paris Cité, INSERM, UMR-1139, Paris, France. [7]National Reference Laboratory for C. difficile, Assistance Publique Hôpitaux de Paris, Hôpital Saint-Antoine, 75012 Paris, France. [8]Institut Universitaire de France, Paris, France. [9]Present address: Institut Pasteur, Université Paris Cité, UMR CNRS 6047, Unité Écologie et Évolution de la Résistance aux Antibiotiques, Paris, France. [10]These authors contributed equally: Marie Royer, Émilie Bertrand, Marius Bredon. e-mail: isabelle.martin-verstraete@pasteur.fr

with a mortality rate of 5–10%[17,19]. These numbers are diminishing in the last few years[4], notably with the increasing use of Fdx, FMT and bezlotoxumab. Although expensive[20,21], these treatments show better clinical efficacy and protection against recurrence than Van and Mtz[22,23]. However, even if limited yet, Fdx resistant strains isolated from patients have been recently described[24–26]. Thus, alternative treatments are still needed, and therapeutic repositioning is one of the considered options, as it allows faster and cheaper development, clinical trials, and commercialization.

Auranofin (AF) is a drug formerly commercialized as Ridauran for its anti-inflammatory properties in the treatment of rheumatoid polyarthritis[27]. Due to more efficient treatments, its use has been gradually stopped in several countries. However, recent studies showed an antibacterial potential for this molecule, with activity against various pathogens including *Staphylococcus aureus*, *Enterococcus* spp. and *Streptococcus* spp., *Helicobacter pylori*, *Mycobacterium tuberculosis*, and *C. difficile*[28–31]. AF was shown to impact growth and survival of *C. difficile* vegetative cells[32,33] and to decrease spore formation and toxin production[29,32]. Accordingly, an AF treatment increases survival in hamster or mouse models of CDI by reducing gut damages[32,34,35].

The mode of action of AF remains unclear. AF has a bactericidal effect against *Mycobacterium* spp. and *Neisseria gonorrhoeae*[28,36,37], but a bacteriostatic effect against *Enterococcus* spp.[38]. AF is known to be an inhibitor of bacterial thioredoxin-reductases (TrxB), as demonstrated on the purified enzymes of *M. tuberculosis* and *S. aureus*[28]. A recent study showed the crucial role of the thiol repair thioredoxin systems in *C. difficile* physiology[39]. Three thioredoxins (TrxAs) and three to four TrxBs are present in *C. difficile* strains. Two TrxBs (TrxB2 and TrxB3) are canonical NADPH-dependent flavin TrxBs (NTRs) while the third one (TrxB1) is a ferredoxin-dependent flavin TrxB (FFTR), an anaerobe-specific class of TrxB. Two thioredoxin systems (TrxA1, TrxA2, TrxB1, TrxB2) are involved in stress response, protecting vegetative cells from exposure to O_2, inflammation-related molecules and bile salts. The TrxA1/B1 system is also present in the spores and contributes to germination and survival to hypochlorite (HOCl), a disinfectant used to eradicate the spores. Finally, the third system (TrxA3/B3) contributes to glycine reduction and sporulation. In addition to the possible TrxB inhibition, AF has a broader effect on thiol homeostasis and selenium metabolism[33]. *C. difficile* possesses two selenoenzymes involved in Stickland metabolism, the proline-reductase, PrdB, and the glycine-reductase, GrdA[40]. The clostridial-specific Stickland pathways allow the production of energy from the degradation of amino acids[41,42]. Various studies show the involvement of Stickland metabolism in *C. difficile* colonization and infection[42,43]. Interestingly, the recycling of the selenoenzyme GrdA is ensured by a dedicated system TrxA3/B3 encoded by the glycine-reductase operon[39,44].

All these studies provide good arguments for the use of AF as a new treatment for CDI. However, several elements are lacking before going through clinical trials. In *C. difficile*, the precise targets of AF and potential resistance mechanisms remain uncharacterized while interactions with molecules produced in the gut during infection and with first-line treatments are not described. Moreover, AF spectrum of action and its impact on the gut microbiota has never been studied. This question is crucial, especially in a context where the gut microbiota is the main barrier against CDIs and recurrences[1,13]. In this work, we studied AF interactions with other therapeutic molecules or with infection-related molecules, addressed the question of potential resistance mechanisms in clinical strains or generated in laboratory, and analyzed the impact of AF on human gut microbiota in vitro.

Results

Role of TrxBs in AF response

Bacterial TrxBs are known to be the first target of AF[28]. The *C. difficile* 630Δ*erm* strain has three *trxB* genes in its genome[39]. We have previously inactivated the *trxB1* and *trxB2* genes in the 630Δ*erm* strain and obtained a double *trxB1/trxB2* mutant[39]. To investigate the role of TrxB in AF tolerance in *C. difficile*, we performed a Minimum Inhibitory Concentration (MIC) assay (Table 1). The MIC of the strain 630Δ*erm* is 0.75 μg mL^{-1}. Single *trxB* mutants had similar MIC to that of the parental strain, while a 2-fold decrease was observed for the double *trxB1/trxB2* mutant. We observed a similar trend using an assay on plates containing sub-inhibitory doses of AF (Fig. 1A, B), with a survival defect only for the double mutant. These results indicate that the inactivation of the genes encoding the two TrxBs involved in stress response increased the susceptibility to AF.

Table 1 | MIC of *trxB* mutants

Strain	MIC auranofin (μg mL^{-1})
WT (630Δ*erm*)	0.750
trxB1	0.750
trxB2	0.750
trxB1/trxB2	0.375

The MIC was determined using the liquid two-fold serial dilution method. The experiment was performed in four biological replicates.

As AF has been shown to have a bactericidal effect on several bacteria[28,36,37], we performed a Minimum Bactericidal Concentration (MBC) experiment (Fig. 1C). We demonstrated that AF have a bactericidal effect on *C. difficile*, with a MBC of 1.5 μg mL^{-1} for the 630Δ*erm* strain. This MBC remained similar in the single *trxB1* and *trxB2* mutants, while the double mutant MBC was 0.75 μg mL^{-1} with a 5-log decrease of survival compared to the parental strain (Fig. 1C). Interestingly, a significant drop of survival was observed at 0.75 μg mL^{-1} for the *trxB1* mutant compared to the WT strain, suggesting that this mutant was more susceptible to AF than the parental strain. No significant differences were observed between the *trxB1* and the *trxB2* mutant. These results confirm that TrxBs are involved in AF tolerance with a slightly more pronounced effect of TrxB1, and strongly suggest that *C. difficile* TrxBs are AF targets.

Impact of the presence of an additional TrxB paralog on AF susceptibility

Not all *C. difficile* strains harbor the same number of *trxB* genes. Indeed, we have recently identified the presence of a fourth *trxB* gene (*trxB4*) widely distributed in *C. difficile* strains from clades 3 and 5[39]. TrxB4, like TrxB1, is a FFTR[45] contrary to TrxB2 and TrxB3 which are NTRs. As we observed a higher susceptibility of the *trxB1* mutant to AF, we investigated the influence of the presence of a second FFTR on AF resistance. The MIC of a panel of clinical strains harboring or not the *trxB4* gene (Supplementary Table 1) was tested. Clade 3 and clade 5 strains carrying the *trxB4* gene were included, but also *trxB4*-positive strains from clade 1 and clade 2 for which most of the strains are not encoding the *trxB4* gene[39]. No significant difference in the MIC of AF was observed between the strains harboring or not the *trxB4* gene (Fig. 1D). In addition, there were no differences in MIC between strains with or without *trxB4* in clades 1 and 2. As *trxB* gene deletion has an impact on MBC, we assessed the MBC of three strains encoding *trxB4*. We used two clinical strains, the E1 (clade 5) and the RT023 strain (clade 3), and the 630Δ*erm* strain harboring a pMTL84121 plasmid carrying the *trxB4* gene from the E1 strain expressed under the control of its own promoter[39]. Both the E1 and the RT027 strains had a MIC of 1.5 μg mL^{-1} (Supplementary Table 1) and a MBC of 3 μg mL^{-1} (Fig. 1E), corresponding to a 2-fold increase compared to the 630Δ*erm* strain. The expression of the *trxB4* gene in the 630Δ*erm* strain did not change neither the MIC nor the MBC. Even though a slight increase in resistance was observed for the two clinical strains encoding TrxB4, our results are not sufficient to conclude that this additional FFTR impacts susceptibility to AF.

Interaction of AF with other antibiotics used for *C. difficile* infection treatment

Another potential resistance mechanism that could be already spread in *C. difficile* strains is cross-resistance with antibiotics of first-line treatments. We evaluated the AF MICs of clinical strains resistant to Mtz or Fdx and of

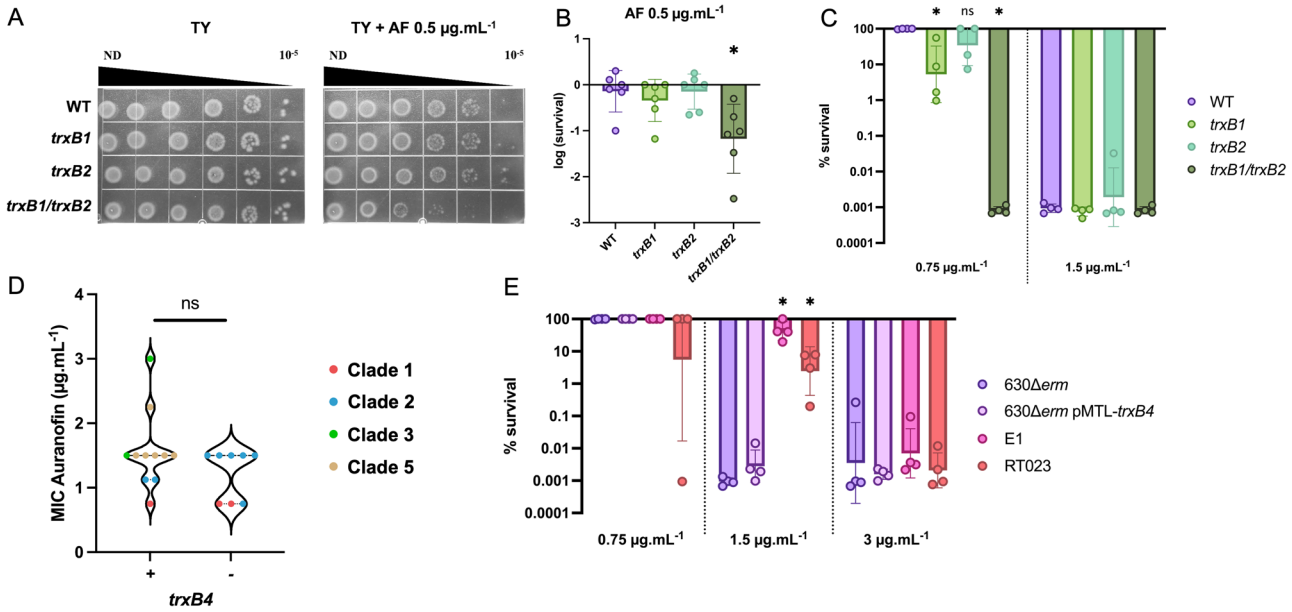

Fig. 1 | Role of TrxBs in AF susceptibility. A, **B** Growth of *trxB* mutants in presence of AF. **A** Culture of 630Δ*erm* was serially diluted and spotted on TY and TY containing AF 0.5 µg mL^{-1}. **B** The survival was calculated by doing the ratio between CFUs with AF and CFUs without AF. Experiment was performed in six biological replicates. Mean and SD are shown. **C** MBCs of *trxB* mutants. MIC experiments were performed and CFUs from inoculum and wells with no visible growth were numerated. Survival was calculated by doing the ratio between the CFUs after and before treatment. Experiment was performed in four biological replicates. Geometric mean and geometric SD are shown. **D** MICs of clinical strains. MICs of clinical strains encoding or not the *trxB4* gene were compared. The clade of each strain is indicated by a color code. The MIC to AF of these different strains carrying or not the *trxB4* gene were indicated in Supplementary Table 1. MICs were performed in four biological replicates. **E** MBC of strains containing or not the *trxB4* gene. MIC experiments were performed on the 630Δ*erm* strain, the 630Δ*erm* strain expressing the *trxB4* gene or on the E1 and RT027 strains, which naturally contain the *trxB4* gene. CFUs from inoculum and wells with no visible growth were numerated. Survival was calculated by doing the ratio between the CFUs after and before treatment. Experiment was performed in four biological replicates. Geometric mean and geometric SD are shown. For survival on plate, one-way ANOVA was performed followed by Tukey's multiple comparison. For MBC, Mann–Whitney tests were used. For the MIC comparison, a Mann–Whitney test was used. * indicates p value < 0.05.

Table 2 | MIC of first-line antibiotic resistant strains

Strain	Drug	Epidemiological cut-off (µg mL^{-1})	MIC 1st ATB (µg mL^{-1})	MIC auranofin (µg mL^{-1})
630Δ*erm*	/	/	/	0.750
CD19-071	Fdx	0.5	16	0.375
CD18-314	Van	2	1.5	1.500
CD19-017			1.5	0.750
CD19-230			1.5	1.500
CD20-059			2	0.750
104-1	Mtz	2	16	1.500
804			4	1.500
861			8	0.750
91861-2			16	0.750
985 642			8	0.750
985 827			8	0.750

The epidemiological cut-off[100] and the MIC for the first-line treatment are indicated. The MIC for AF was determined using the liquid two-fold serial dilution method. The experiment was performed in four biological replicates.

strains with a decreased sensitivity to Van (Table 2). The MICs of these strains were between 0.375 and 1.5 µg mL^{-1}, corresponding to a 2-fold change or less compared to the 630Δ*erm* reference strain. The absence of higher MIC of AF for clinical resistant strains indicates that no cross-resistance was detected. We also tested the synergy of AF with the three antibiotics used for CDI treatments using the Fractional Inhibitory Concentration (FIC) method[46] (Table 3). We obtained values between 0.5 and 1 for Fdx and Mtz, suggesting an additive effect with AF. For Van, the FIC value was between 1 and 4 indicating no interaction with AF. Our results suggest that no cross-resistance mechanism is already present in clinical

Table 3 | FIC indexes of AF and first-line treatments

Antibiotic	FIC index	Conclusion
Fdx	0.61	Additive effect
Van	1.64	No interaction
Mtz	0.91	Additive effect

The FIC index was determined using AF and Fdx, Van or Mtz. FIC < 0.5 indicates synergy, 0.5 < FIC < 1 indicates additive effect, 1 < FIC < 4 indicates no interaction and 4 < FIC indicates antagonism. The experiment was performed in four replicates.

strains of *C. difficile* and indicate that no antagonism exists between AF and the first-line treatments against CDIs. The risks of using a two-drug therapy with AF are therefore limited.

Generation of adaptive mutations through long-term exposure to AF

In order to study the appearance of resistance in vitro, we tried to generate mutations conferring a decreased susceptibility to AF *via* two strategies. We first used a screening of spontaneous resistant clones by plating cultures of strain 630Δ*erm* on plates containing high doses of AF (5 and 10 μg mL^{-1}). After 5 to 7 days at 37 °C, clones were visible on plates but the MIC of most of these clones remained between 0.75 and 1.5 μg mL^{-1}. Three clones had an increased MIC (3 to 6 μg mL^{-1}). However, when sequenced, no mutations were identified, suggesting an absence of stability of the selected mutations.

The second approach was a long-term exposure to sub-inhibitory dose of AF with iterative MIC experiments (Fig. 2A). After a first MIC experiment, the well with visible growth at the highest concentration of AF was used to prepare the inoculum for the next MIC experiment. This method allows an adaptive increase of the AF dose over time. We performed this experiment for 30 days and followed the MIC of the 630Δ*erm* and the E1 strains. The MIC of both strains increased slightly over the experiment. The maximum MIC values reached during the experiment were 3 and 6 μg mL^{-1} obtained for the 630Δ*erm* and E1 strains, respectively, corresponding to a 4-fold increase. Importantly, this increase was not stable over time regardless of the strain, with variations of the MIC from day to day. Finally, the E1 strain had a higher MIC over time than the 630Δ*erm* (two-way ANOVA, p value = 0.03), confirming that the E1 strain is more tolerant to AF than the 630Δ*erm* strain (Supplementary Table 1 and Fig. 2A).

To identify selected mutations, we sequenced at day 30 the evolved populations, 4 replicates of the E1 strain and 3 biological replicates for the 630Δ*erm* strain. Additionally, the replicate 3 of the E1 strain was also sequenced at day 10, corresponding to the first day when a replicate reached a MIC of 6 μg mL^{-1}. Although several mutated genes have been identified (Supplementary Table 2), two of them were mutated in independent populations. Mutations in the *rsbW* gene were identified in all the 630Δ*erm* replicates and in the third replicate of the E1 strain, both at day 10 and day 30. RsbW is the anti-sigma factor of σ^B, the sigma factor of the general stress response[47]. Three mutations were different non-synonymous point mutations at different positions of the *rsbW* gene. The fourth mutation was an insertion of a T at position 17 over 408 that introduces an early stop codon leading to the production of a truncated RsbW protein of 17 amino acids instead of 135. Finally, two 630Δ*erm* replicates presented two different

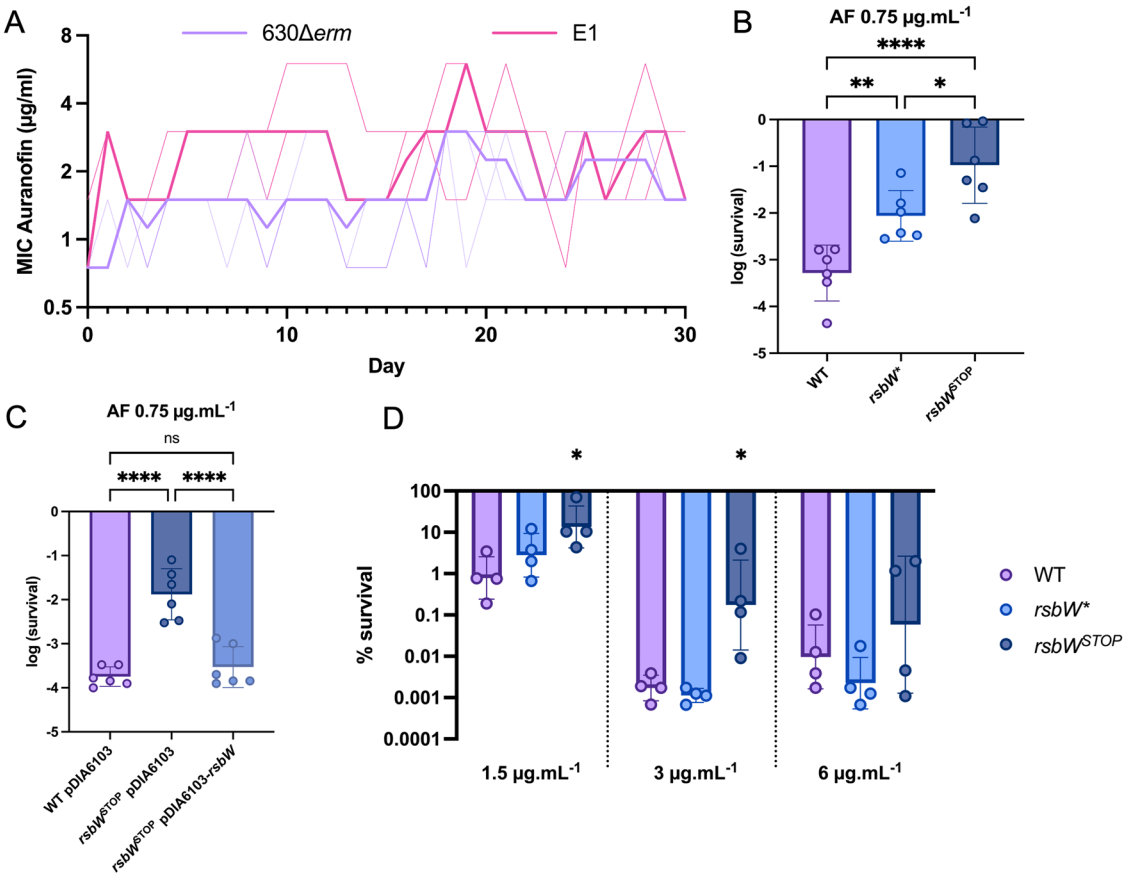

Fig. 2 | Generation and characterization of adaptative mutation to AF. **A** Evolution of AF MIC during long time exposure. MIC experiments were performed on the 630Δ*erm* and the E1 strain over 30 days. Every day, the bacterial suspension with visible growth at the highest AF concentration was used to prepare a new MIC experiment after a 1:100 dilution. MIC was recorded daily. Thin lines represent the four biological replicates of each strain, thick line represents the median. **B**, **C** Survival of mutated strains. Cultures of 630Δ*erm*, *rsbW** and *rsbW*^{STOP} strains (**B**) or cultures of 630Δ*erm* pDIA6103, *rsbW*^{STOP} pDIA6103 and *rsbW*^{STOP} pDIA6103-*rsbW* strains (**C**) were serially diluted and spotted on TY and TY containing AF at 0.75 μg mL^{-1}. The survival was calculated by doing the ratio between CFUs with AF and CFUs without AF. Experiments were performed in six biological replicates. **D** MBC of the 630Δ*erm, rsbW** and *rsbW*^{STOP} strains. MIC experiments were performed and CFUs from inoculum and wells with no visible growth were numerated. Survival was calculated by doing the ratio between the CFUs after and before treatment. Experiments were performed in four biological replicates. Geometric mean and geometric SD are shown. For survival on plate, one-way ANOVA was performed followed by Tukey's multiple comparison. For MBC, Mann–Whitney tests were used. * indicates p value < 0.05, ** <0.01, *** <0.001 and **** <0.0001.

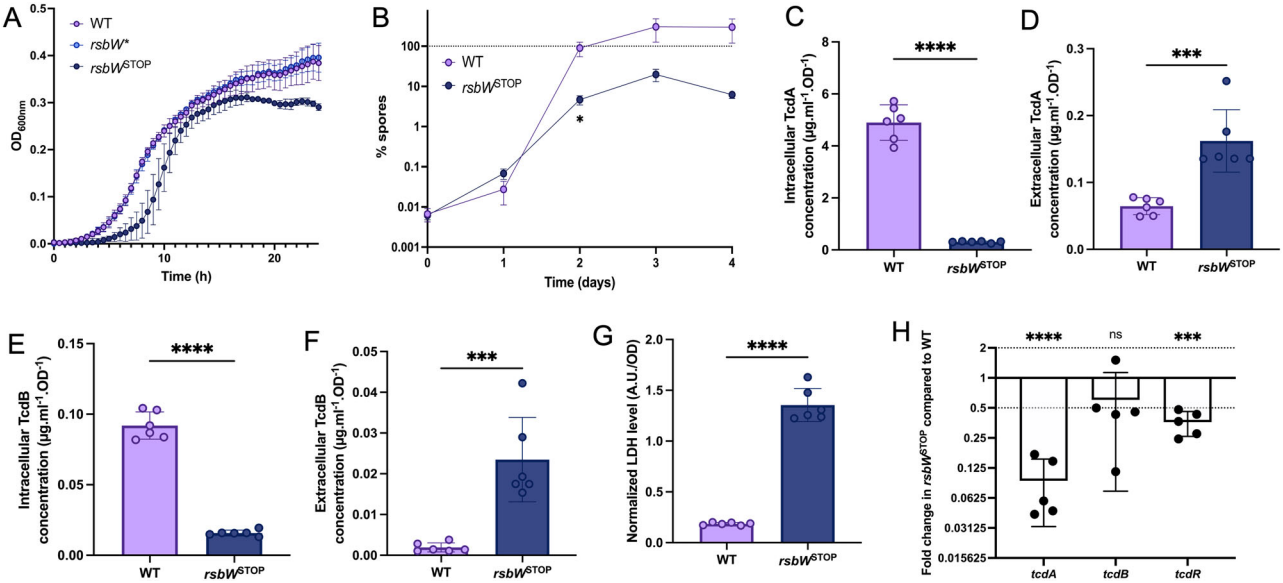

Fig. 3 | Impact of the *rsbW*^{STOP} mutation on *C. difficile* physiology. A Growth of the *rsbW* mutants. Growth of 630Δ*erm, rsbW** and *rsbW*^{STOP} strains was assessed by following OD_{600nm} in 96-well plates in TY medium. Experiments were performed in five technical and three biological replicates. Mean and SD are shown. **B** Sporulation of the *rsbW*^{STOP} strain. Sporulation rate was evaluated by serially diluting a culture and plating before (total cells) and after (spores) ethanol shock. Sporulation rate was evaluated by calculating the ratio between spores and total CFUs. Mean and SEM are shown. **C**–**F** Toxin production. One ml of a 24 h culture was harvested and centrifuged. Supernatant was used for extracellular toxins quantification. Pellet was lysed to determine intracellular toxin levels. Sandwich ELISAs were performed to evaluate **C**, **D** TcdA and **E**, **F** TcdB concentrations in **C**, **E** intracellular and **D**, **F** extracellular fractions. Toxin amount was normalized using the OD_{600nm} of the culture. Experiment was performed on six biological replicates. Mean and SD are shown. **G** Extracellular LDH in the WT strain and *rsbW*^{STOP} mutant. One ml of a 24 h culture was harvested and centrifuged. LDH present in the supernatant was quantified and normalized by the OD_{600nm} of the culture to evaluate cell lysis. Experiment was performed on six biological replicates. Mean and SD are shown. **H** Expression of toxin-related genes. Expression of genes was compared by qRT-PCR between the WT and *rsbW*^{STOP} strains. Experiment was performed on five biological replicates. Mean and SD are shown. For sporulation, multiple *t*-tests were used to compare the rate of sporulation every day. For toxin quantification, unpaired *t*-tests were performed. For LDH assay, unpaired *t*-test was performed. For qPCR, one sample *t*-tests were used with comparison of the fold change to 1. * indicates p value < 0.05, ** <0.01, *** <0.001 and **** <0.0001.

non-synonymous point mutations in the *CD3089* gene encoding a phosphotransferase system specific for trehalose[48].

Characterization of the mutations on AF susceptibility

To study the impact of the mutations in the *rsbW* and *CD3089* genes on AF susceptibility, we constructed a *CD3089::erm* mutant in the 630Δ*erm* background and we used two *rsbW* mutants of the 630Δ*erm* strain obtained from the evolution experiment (Supplementary Table 2). The 630Δ*erm* replicate 2, mentioned as the *rsbW** strain, has a D37Y modification in RsbW. The 630Δ*erm* replicate 3, mentioned as the *rsbW*^{STOP} strain, has an early stop codon in the *rsbW* gene but also contains a F228L mutation in the *CD3089* gene. To complement the *rsbW*^{STOP} mutation, we used a plasmid carrying the *rsbW* gene expressed under the control of its own promoter[47].

First, no differences of MIC were observed for the different mutants compared to the parental strain 630Δ*erm* (Supplementary Table 3). Since the expression of the *CD3089* gene is induced by trehalose[48], we performed MIC and survival assays in presence of 10 or 100 mM of trehalose. Identical MICs were obtained for the WT strain and the *CD3089::erm* mutant in all the conditions tested (Supplementary Table 3), while the survival on plates containing 0.75 µg mL^{-1} AF was similar for these two strains in absence or in presence of trehalose (Supplementary Fig. 1A). In contrast, we observed an increased survival upon exposure to 0.75 µg mL^{-1} of AF for both strains containing a mutation in the *rsbW* gene compared to the parental strain, with a greater effect for the *rsbW*^{STOP} strain than for the *rsbW** strain (Fig. 2B). Plasmid complementation of the *rsbW*^{STOP} mutant with the WT copy of the *rsbW* gene restored AF susceptibility (Fig. 2C). These results confirmed that mutations in the *rsbW* gene were responsible for increased survival to AF and suggested that the *CD3089* gene is not involved in this phenotype. Finally, we performed MBC assays of the four strains (Fig. 2D and Supplementary Fig. 1B). The *rsbW** and the *CD3089::erm* strains had no differences of survival compared to the 630Δ*erm* strain. However, the MBC of the *rsbW*^{STOP} was 6 µg mL^{-1} instead of 3 µg mL^{-1} for the parental strain. Altogether, our results indicated that the inactivation of *rsbW*, decreases AF bactericidal activity, although it does not confer resistance.

Impact of the *rsbW*^{STOP} mutation on *C. difficile* physiology

We evaluated the impact of the *rsbW* mutations on key steps of the bacterium physiology. We first performed growth curves of the strains (Fig. 3A). No differences were observed between the WT and the *rsbW** strain, but the *rsbW*^{STOP} strain displayed a longer lag phase and a reduced growth yield compared to the WT strain (Fig. 3A). This growth defect was exacerbated in a peptone-containing medium (Pep-M), a less rich medium (Supplementary Fig. 2A). We then assessed the sporulation efficiency of the *rsbW*^{STOP} strain (Fig. 3B). The *rsbW*^{STOP} strain produced significantly less spores after 48 h compared to the parental strain and never reached 100% of sporulation, contrary to the WT strain. Finally, we tested the production of toxins (Fig. 3C–F). The intracellular levels of TcdA and TcdB were significantly reduced in the *rsbW*^{STOP} strain compared to the parental strain (Fig. 3C, E). By contrast, the extracellular levels of toxins, although way lower than the intracellular levels, were higher in the *rsbW*^{STOP} strain (Fig. 3D, F). The increased levels of extracellular toxin are probably due to an increased lysis since more lactate dehydrogenase, a cytoplasmic protein used as lysis control, was detected in the supernatant of the *rsbW*^{STOP} strain (Fig. 3G). Consistently with the decreased total amount of toxins produced, we also observed a downregulation of the expression of the *tcdA* and *tcdB* genes by qRT-PCR in the *rsbW*^{STOP} strain, although not significant for *tcdB* (Fig. 3H). Since *tcdR* is also downregulated in the *rsbW*^{STOP} strain, we assumed that the transcriptional control of *tcdA* and *tcdB* expression by RsbW is mediated via TcdR, the specific sigma factor of *tcdA* and *tcdB* transcription[49].

Altogether, our results indicate that the *rsbW*^{STOP} mutation has a strong impact on *C. difficile* physiology with a modified growth, an increased cell lysis, a reduced sporulation efficiency, and a drop in toxin production.

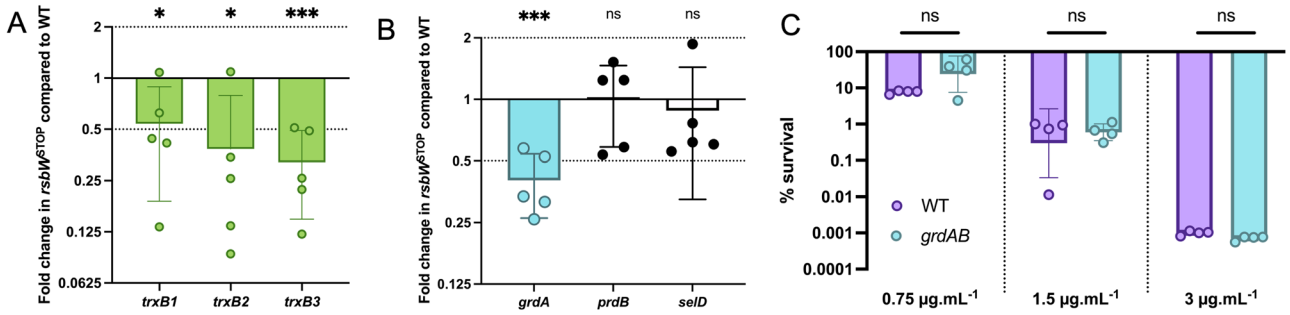

Fig. 4 | Impact of the *rsbW*^{STOP} mutation on gene expression and role of *grdAB* in AF survival. A, **B** Gene expression in the *rsbW*^{STOP} strain. Expression of the *trxB* genes (**A**) and of the *grdA*, *prdB* and *selD* genes (**B**) was measured by qRT-PCR in WT and *rsbW*^{STOP} strains. Experiments were performed in five biological replicates. Mean and SD are shown. **C** MBC of the Δ*grdAB* mutant. A MIC experiment was performed and CFUs from inoculum and wells with no visible growth were numerated. Survival was calculated by doing the ratio between the CFUs after and before treatment. Experiment was performed in four replicates. Geometric mean and geometric SD are shown. For qRT-PCR, one sample *t*-tests were used with comparison of the fold change to 1. For MBC, Mann–Whitney tests were used. * indicates p value < 0.05 and *** <0.001.

Characterization of the *rsbW*^{STOP} mutation

We thus wanted to dig into the mechanism of the decreased AF susceptibility of the *rsbW*^{STOP} strain. RsbW is the anti-sigma factor of σ^B, the sigma factor of the general stress-response[47]. σ^B controls the expression of a large set of genes involved in stress response, including the *trxA1-trxB1* operon and the *trxB2* gene[39,50]. We therefore compared the expression of the *trxB* genes in the *rsbW*^{STOP} and WT strains by qRT-PCR (Fig. 4A). We found that the three *trxB* genes were downregulated in the *rsbW*^{STOP} strain compared to the WT strain, suggesting a positive regulation by RsbW. Since *trxB1* and *trxB2* are transcribed from a promoter recognized by σ^B[39,50,51] and because RsbW is the anti-σ^B, we expected that *trxB1* and *trxB2* gene expression would be upregulated in the *rsbW*^{STOP} strain. We can exclude that this unexpected result is due to a polar effect of the *rsbW*^{STOP} mutation on the *sigB* gene located downstream (Supplementary Fig. 2B)[47] as we did not observe differences in the expression of the *sigB* gene in the *rsbW*^{STOP} strain compared to the WT strain (Supplementary Fig. 2C). All these data suggest that RsbW, despite being described as the anti-σ^B, may have another function and might also control genes that do not belong to the σ^B regulon such as *trxB3*. This hypothesis is consistent with a study performed on a Δ*rsbW* mutant in the R20291 strain indicating that most of the genes positively controlled by σ^B are not upregulated in a *rsbW* mutant[52].

The decreased susceptibility of the *rsbW*^{STOP} strain to AF is not due to an overexpression of *trxB* genes. Another possible target of AF are selenoenzymes[33]. *C. difficile* selenoproteins are the Stickland enzymes PrdB and GrdA, whose synthesis relies on the selenophosphate synthetase, SelD[40]. In the R20291 Δ*rsbW* mutant, the expression of both the *grd* and *prd* operons is strongly downregulated, including the genes encoding for PrdB and GrdA[52]. In the *rsbW*^{STOP} strain, we found that the expression of *grdA* was significantly downregulated compared to the WT strain, while the *rsbW* mutation had no effect on the expression of the *prdB* or the *selD* gene (Fig. 4B). To see if the downregulation of *grdA* contributes to the tolerance of the *rsbW*^{STOP} strain, we performed an MBC assay on a Δ*grdAB* mutant (Fig. 4C). No differences were observed between the Δ*grdAB* mutant and the WT strain, suggesting that the downregulation of *grdA* expression alone is not sufficient to decrease AF susceptibility. However, this downregulation can explain, at least partly, the sporulation defect of *rsbW*^{STOP} strain, as *grdAB* has been shown to contribute to sporulation[39,53].

Synergy of AF with inflammation-associated molecules

A loss of efficiency of a treatment at the infection site can also be due to inactivation of the antibiotic by molecules produced by the host or the microbiota, or by antagonistic interactions. CDI is associated with microbiota dysbiosis leading to an increase of O_2-tensions in the gastrointestinal tract and with an intense inflammation leading to the production of antibacterial compounds by immune cells[8,9,54,55]. To evaluate the impact of such molecules on AF activity, we tested the effect of a sub-inhibitory concentration of AF (0.5 µg mL^{-1}) in presence of different molecules of the inflamed gut (Fig. 5). Combining a sub-inhibitory dose (0.1%) of HOCl with AF (Fig. 5A) led to a complete inhibition of *C. difficile* growth on plates. An inhibition was also observed with DEA-NONOate, a nitric oxide (NO) donor, at 750 µM (Fig. 5B). These results confirmed that the presence of inflammation-related molecules potentializes the effect of AF on *C. difficile*. Compared to anaerobiosis, we observed a more drastic effect of AF at a low physiological O_2-tension of 0.4%[56,57] (Fig. 5C). Interestingly, when we exposed *C. difficile* to a lethal dose of Mtz (1.5 µg mL^{-1}) at 0.4% O_2 (Fig. 5D), we observed a decrease of the activity of Mtz. Altogether, our results suggest that in opposition to Mtz, AF activity on *C. difficile* is increased in presence of infection-related stress molecules.

Effect of AF on human gut microbiota

Both CDIs and recurrences are linked to microbiota dysbiosis[3,13], underlying importance to analyze the impact of *C. difficile* treatments on gut microbiota. The impact of AF on human gut microbiota has not been studied yet, and its spectrum of action is poorly characterized. To address these questions, we used MiPro, an in vitro microbiota model, which allows the culture of human gut microbiota in 96-well plates[58]. This model can allow to study the impact of molecules on the microbiota[59]. We evaluated the effect of three doses of AF (3 ; 30 and 300 µg mL^{-1} corresponding to 4; 40 and 400x the MIC) on four individual frozen biobanked fecal microbiota from healthy subjects as previously described[60]. Van, a *C. difficile* treatment known to perturbate the microbiota[61], was used as a control. The dose used for Van (500 µg mL^{-1}) corresponds to 300x to 500x the MIC[62] and to fecal concentration found in patients treated four times a day with an oral dose of 125 mg following recommendations[63]. Such data are lacking for AF, but we tested a range of concentrations (from 3 to 300 µg mL^{-1}) that includes the dose found in patients stools following a treatment for rheumatoid polyarthritis (5 µg mL^{-1})[64].

After 48 h of culture, microbiota composition was analyzed by 16S sequencing. A treatment with Van significantly induced a decreased Alpha-diversity, as shown by the Shannon index (Fig. 6A), while a trend of decrease in diversity was observed with AF in a dose-dependent manner. A Spearman's correlation (Fig. 6B) highlighted a significant negative correlation between AF doses and Alpha-diversity (Chao1 index, p value = 0.0014), indicating that AF also impacts microbiota composition.

We therefore analyzed which bacteria were impacted by the various treatments (Fig. 7 and Supplementary Data). Van induced a significant decrease in abundance of *Bacteroidaceae*, *Lachnospiraceae*, *Barnesiellaceae* and *Tannerellaceae*, while AF only significantly impacted *Bacteroidaceae* abundance at the highest dose (Fig. 7A and Supplementary Data). However, Spearman's correlation pointed out some effects of AF treatments (Fig. 7B). There were significant negative correlations between AF doses and

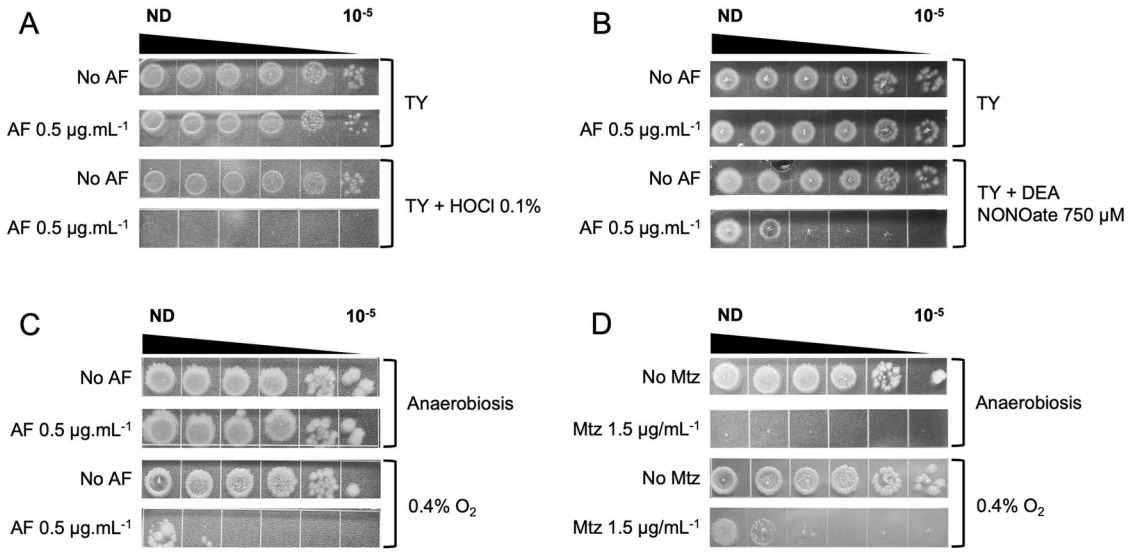

Fig. 5 | Impact of infection-related molecules on AF activity. A, **B** Synergy of AF with molecules produced during inflammation. Culture of 630Δ*erm* was serially diluted and spotted on TY with or without AF 0.5 µg mL^{-1} and with or without **A** HOCl 0.1% or **B** DEA NONOate 750 µM. **C** Synergy of AF with O_2 and **D** antagonism of Mtz and O_2. Culture of 630Δ*erm* was serially diluted and spotted in duplicate on TY Tau plates with or without AF 0.5 µg mL^{-1} (**C**) and with or without Mtz 1.5 µg mL^{-1} (**D**). Plates were incubated either in anaerobiosis or at 0.4% O_2. Photos are representative of four independent biological replicates.

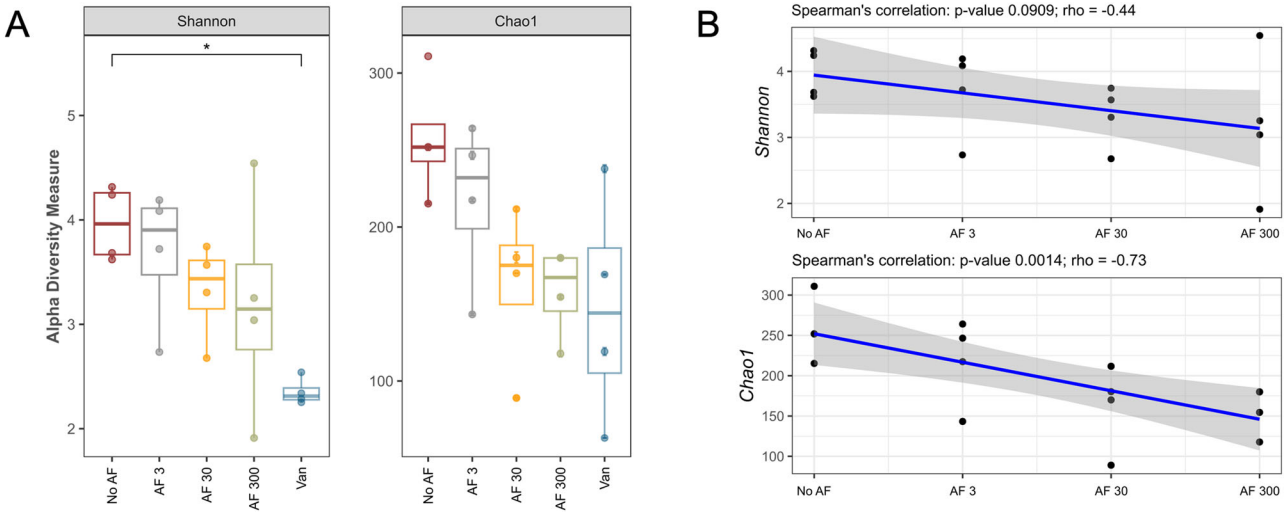

Fig. 6 | Effect of AF on human gut microbiota cultured diversity. A Alpha diversity indices (Shannon and Chao1) calculated from the raw taxonomic tables after 48 h of treatment with AF (3, 30 or 300 µg mL^{-1}) or Van (500 µg mL^{-1}). Kruskal–Wallis tests with Dunn's test post hoc (Benjamini–Hochberg *p* value correction method) were used to compare the groups. * indicates *p* value < 0.05. **B** Spearman's correlation of the dose of AF and Alpha-diversity indices.

abundance of *Bacteroidaceae*, *Oscillospiraceae*, *Lachnospiraceae* and *Barnesiellaceae*, suggesting that AF inhibits the growth of these organisms in the human microbiota. Moreover, a positive correlation was shown for *Enterobacteriaceae*, indicating that AF treatment favors their presence. Altogether, our results indicate that AF has a lesser impact on human microbiota than Van, even if it still impacts the microbiota composition.

Discussion

In this work, we provided new elements for the use of AF as a possible treatment for CDI. AF has been demonstrated in various study to protect against CDI in animal models[32,34,35]. AF inhibits *C. difficile* growth but also sporulation and toxin production, both in vivo and in vitro[32]. We demonstrated that AF has a bactericidal activity on *C. difficile*, as observed in other bacteria[28,36]. In addition, we showed that the efficiency of AF on *C. difficile* increases in presence of infection-related metabolites such as HOCl and NO or low physiological O_2 tension. These molecules are known to post-translationally modified thiols through oxidation or S-nitrosylation[65,66]. The TrxBs involved in thiol repair are necessary for HOCl, O_2 and NO survival in *C. difficile*[39]. Thus, the likely inhibition of TrxB activity by AF, which has been demonstrated for the TrxB of *M. tuberculosis* and *S. aureus*[28], probably results in an increased susceptibility of *C. difficile* to HOCl, O_2 and NO in the presence of AF. These results suggest that AF would have an increased activity against *C. difficile* at the site of infection during inflammation and dysbiosis.

Consistent with a TrxB inhibition by AF, we demonstrated that a double *trxB1/trxB2* mutant was more susceptible to AF. In addition, survival of a *trxB1* mutant to AF at 0.75 µg mL^{-1} was also significantly reduced compared to the WT strain, which was not the case for the *trxB2* mutant. This result needs to be confirmed, as there was no significant difference between the *trxB1* and the *trxB2* mutants, but it suggests that the NTR TrxB2 is slightly more susceptible to AF inhibition than TrxB1, which is a

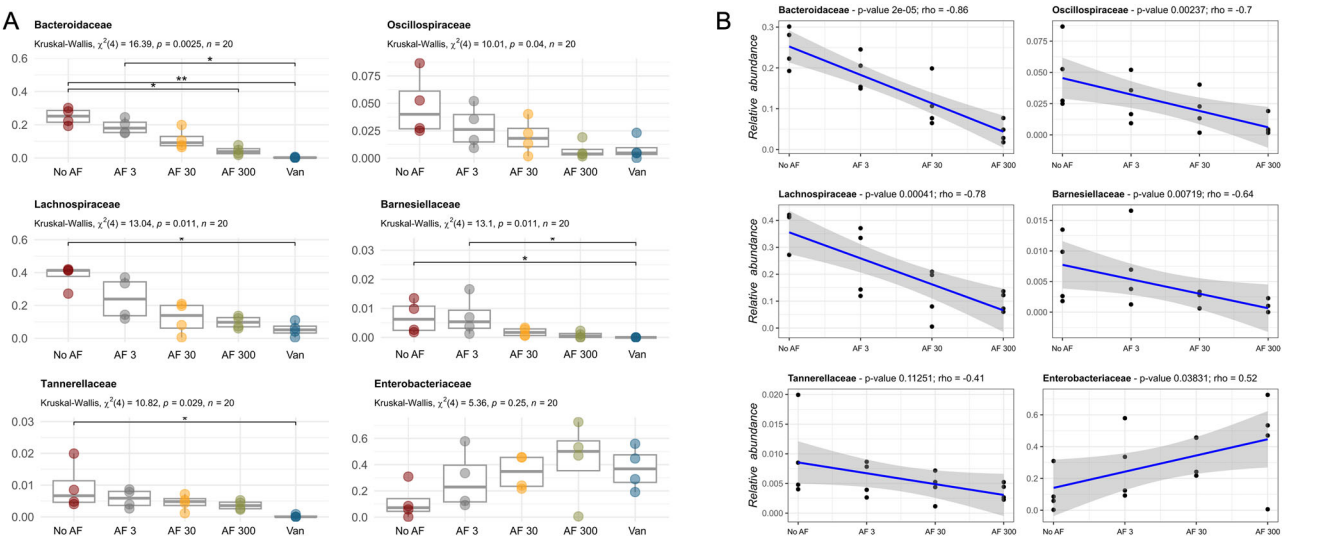

Fig. 7 | Effect of AF on specific bacterial families. A Relative abundance of different bacterial families after 48 h of treatment with AF (3, 30 or 300 µg mL^{-1}) or Van (500 µg mL^{-1}). Kruskal–Wallis tests with Dunn's test post hoc (Benjamini–Hochberg *p* value correction method) were used to compare the groups. * indicates *p* value < 0.05, ** <0.01. **B** Spearman's correlation of the dose of AF and relative abundances of bacterial families.

FFTR, a class of TrxB specific of anaerobes[45]. Some strains of *C. difficile* harbor a second FFTR, TrxB4[39]. The presence of the *trxB4* gene mainly found in clade 3 and clade 5 strains, did not significantly decrease susceptibility to AF. Interestingly, clade 5 strains have been demonstrated to be more tolerant to ebselen[67], another TrxB inhibitor[68], although the link with the presence of *trxB4* has not been established.

The slight effect of the inactivation of both *trxB1* and *trxB2* on AF susceptibility with only a significant two-fold change in MIC and MBC, suggests that either TrxB3 compensates the inactivation of the two other enzymes, or that there are other AF targets in the cell. The other known targets in *C. difficile* are the selenoenzymes, GrdA and PrdB, which are crucial for *C. difficile* physiology[42,53,69]. AF disrupts selenium metabolism and the production of these selenoenzymes[33]. The selenium-mediated mechanism by which AF inhibits *C. difficile* is still unclear, as a recent study showed that mutants lacking selenoproteins were as susceptible to AF as the parental strain[70]. However, it is to note that only MIC assays were performed in this study, whereas we observed decreased susceptibility to AF only through MBC assays. The multiplicity of AF targets probably explains why the apparition of resistance to AF is limited in *C. difficile*. In *S. aureus*, the modified TrxB protein with G13T and G139A substitutions leads to a 512-fold increase of the MIC of AF[71]. However, *S. aureus* has a unique TrxB[72] and no selenoproteins. We identified a unique mutation decreasing AF susceptibility that corresponds to the synthesis of a truncated inactivated form of RsbW, the anti-sigma factor of σ^B[47,50]. As σ^B controls the expression of two *C. difficile trxB* genes[39], we first hypothesized that this tolerance was due to their derepression and thus, an increase of the amount of TrxB in the cell. However, *rsbW* inactivation rather decreased *trxB* gene expression. Another change in the *rsbW*^{STOP} mutant is a decreased expression of *grdA*, but we were not able to demonstrate that this downregulation was correlated with a decreased susceptibility. The mechanism involved in the decreased susceptibility to AF in the mutants inactivated for *rsbW* remains to be identified. In addition, we showed that the *rsbW*^{STOP} mutation strongly impacts *C. difficile* physiology and maybe also pathogenesis by decreasing toxin production and spore formation. These results are in agreement with a previous study on a Δ*rsbW* mutant in a ribotype 027 strain[52]. It suggests that if such a mutation appears in vivo, the pathogenesis and thus the symptoms of the infection would probably diminish, as observed in the case of Fdx resistance[25]. Consistently, the Δ*rsbW* mutant of a 027 ribotype strain is less virulent in a *Galleria* model of infection[52].

For CDIs, the impact of a treatment on the microbiota is crucial, as it is a major risk factor of recurrence[13]. We evaluated the effect of AF on human gut microbiota composition using an in vitro microbiota model. We showed that AF impacts microbiota diversity in a lesser extent than Van. Interestingly, we observed an overlap between Van- and AF-impacted bacteria (Supplementary Data). This result suggests that these two molecules have a rather similar spectrum of action, even if their molecular targets in the cell are completely different[73]. Our in vitro microbiota experiment also provides clues on the spectrum of action of AF, which is still poorly characterized. For antibacterial purpose, AF was shown to affect several Firmicutes, *Mycobacterium* spp. and *H. pylori*[28,38]. Here, we demonstrated that AF decreases the abundance of the *Oscillospiraceae* and *Lachnospiraceae* Firmicutes[74], confirming the general susceptibility of this phylum to AF. This molecule also impacts the abundance of two members of the *Bacteroidales* order, *Bacteroidaceae* and *Barnesiellaceae*[75]. An effect of AF on *Bacteroidales* has been previously demonstrated in vitro[76]. Interestingly, *Bacteroidales*, as many Firmicutes, *Mycobacterium* spp. and *H. pylori*, lack the Glutaredoxin (Grx) system[77–79]. The Grx system is an alternative system for disulfide bond exchange and thiol repair that uses glutathione, a Grx protein and a GSH-reductase[80]. There is a partial functional redundancy between this alternative system for thiol homeostasis and the thioredoxin system[81–83]. The Grx system is widespread in Gram-negative bacteria[83], which are mostly not susceptible to AF[84]. Our results therefore suggest that the lack of Grx system is the reason for AF-susceptibility. This hypothesis has been proposed to explain susceptibility to ebselen, another TrxB inhibitor[68], and is supported by our observation of an increase of abundance of *Enterobacteriaceae* in the microbiota in the presence of AF.

Altogether, our study provides new elements for the use of AF as a CDI treatment. We showed that AF likely targets the TrxBs of *C. difficile* in addition to the selenoenzymes of the cell[33]. This multiplicity of targets leads to a low rate of resistance apparition, and the only mutation that we identified decreasing AF susceptibility strongly impacts *C. difficile* physiology. We also demonstrated no cross-resistances nor negative interactions with the first-line treatments for CDIs. The clinical relevance of synergy assays is still debated[46], but these results suggest that a dual therapy using AF and a first-line treatment should be tested in animal models, before being used in clinics if the results are conclusive. Finally, we provide new elements to identify the spectrum of AF and to characterize its impact on gut microbiota. More studies are required to characterize the impact of AF on human gut microbiota. 16S microbiota analysis, with a characterization of bacterial diversity at the family level, is a first approach. Metagenomics approaches would be a source of additional information about diversity but also

functions that are lost with an AF treatment[85]. Assessing the effect of AF on the microbiota on human subjects would also consider the effect of the immune system, while the MiPro system that we used allows the study of human microbiota and to get rid of the effects of absorption and stomach passage.

Methods

Bacterial strains and culture media

C. difficile strains and plasmids used in this study are listed in Supplementary Table 4. *C. difficile* strains were grown anaerobically (5% H_2, 5% CO_2, 90% N_2) in TY (Bacto tryptone 30 g L^{-1}, yeast extract 20 g L^{-1}, pH 7.4), in Brain Heart Infusion (BHI; Difco), or in Pep-M (Proteose peptone No.2 40 g L^{-1}, Na_2HPO_4 5 g L^{-1}, KH_2PO_4 1 g L^{-1}, NaCl 2 g L^{-1}, $MgSO_4$ 0.1 g L^{-1}). For solid media, agar was added to a final concentration of 17 g L^{-1}. When necessary, thiamphenicol (Tm, 15 µg mL^{-1}), cefoxitin (Cef, 25 µg mL^{-1}) and erythromycin (Erm, 2.5 µg mL^{-1}) were added to *C. difficile* culture. *E. coli* strains were grown in LB broth. When indicated, ampicillin (Amp, 100 µg mL^{-1}) and chloramphenicol (Cm, 15 µg mL^{-1}) were added to the culture medium. When indicated, the spore germinant taurocholate (Tau) was added in plates at 0.05%.

The MiPro culture medium was composed of 2.0 g L^{-1} peptone water, 2.0 g L^{-1} yeast extract, 0.5 g L^{-1} L-cysteine hydrochloride, 2 mL L^{-1} Tween 80, 5 mg L^{-1} hemin, 5 µL L^{-1} vitamin K1, 1.0 g L^{-1} NaCl, 0.4 g L^{-1} K_2HPO_4, 0.4 g L^{-1} KH_2PO_4, 0.1 g L^{-1} $MgSO_4 \cdot 7H_2O$, 0.1 g L^{-1} $CaCl_2 \cdot 2H_2O$, 4.0 g L^{-1} $NaHCO_3$, 4.0 g L^{-1} porcine gastric mucin, 0.25 g L^{-1} sodium cholate, and 0.25 g L^{-1} sodium chenodeoxycholate.

Construction of *C. difficile* strains

All primers used in this study are listed in Supplementary Table 5. The *CD3089*::*erm* mutant was obtained by using the ClosTron gene knockout system as previously described. The PCR product generated by overlap extension that can facilitate intron retargeting to *CD3089* was cloned between the HindIII and BsrG1 sites of pMTL007-CE5 to obtain pDIA7274. This plasmid introduced in the HB101/RP4 *E. coli* strain was then transferred by conjugation into the 630Δ*erm* strain. Transconjugants selected on BHI plates supplemented with Tm and *C. difficile* selective supplement (SR0096, Oxoid) were restreaked into new BHI plates containing Cef and Tm. The mutant was then selected by restreaking into BHI plates containing Cef and Erm.

For the construction of the *rsbW* complementation plasmid, pDIA6325, a derivative of pDIA6103 containing the promoter of the *CD0007-sigB* operon and the *sigB* gene was digested by StuI and BamHI. The *rsbW* gene was amplified by PCR using oligonucleotides NK211 and NK212. The PCR product was cloned between the StuI and BamHI of pDIA6325 replacing the *sigB* gene by *rsbW* to produce pDIA7275. In this plasmid, the *rsbW* gene is expressed under the control of the promoter of the *CD0007-sigB* operon (Supplementary Fig. 2B). This plasmid was transferred by conjugation into the *C. difficile* $rsbW^{STOP}$ strain.

MIC, FIC and MBC experiments

The MIC of AF was determined by broth microdilution containing 2-fold serial dilution of AF in TY medium. After inoculation with a bacterial suspension adjusted to an OD_{600nm} of 0.05, plates were incubated for 24 h at 37 °C in an anaerobic atmosphere. The MIC was recorded as the lowest concentration of antibiotic that inhibited visible growth of the microorganism. Experiment was performed in four biological replicates.

For MBC experiments, MIC assays were performed. The 0.05 initial inoculum was serially diluted and plated on TY agar for numeration of colony forming units (CFUs). After incubation of the MIC plate, wells with absence of visible growth were serially diluted and plated for numeration of CFUs. Survival was determined by doing the ratio between the CFUs after AF exposure and the CFUs in the inoculum. The MBC is defined as the concentration for which less than 0.1% survival is observed. Experiment was performed in four replicates.

FIC experiments were performed as MIC assays, with two gradients of 2-fold serial dilution of AF and Fdx, Van or Mtz. Experiment was performed in four replicates. The FIC index was calculated using the following formula:

$$FIC = FIC_A + FIC_B = \frac{MIC_{A\ with\ B}}{MIC_{A\ alone}} + \frac{MIC_{B\ with\ A}}{MIC_{B\ alone}}$$

Equation (1). FIC index calculation. From ref. 46.

Survival on antibiotic-containing plates

After growth, cultures were serially diluted (non-diluted to 10^{-5}) and 5 µl of each dilution were plated on antibiotic-containing plate and on TY control plate. To test survival to AF, TY agar plates containing 0.5 or 0.75 µg mL^{-1} of AF were used. For synergy experiments with O_2, TY Tau plates were prepared in duplicate and incubated either in anaerobiosis or in the presence of 0.4% of O_2, with either 0.5 µg mL^{-1} of AF or 1.5 µg mL^{-1} of Mtz. For other synergy assays, AF was used at 0.5 µg mL^{-1} and DEA NONOate and HOCl were used at 750 µM and 0.1%, respectively. The experiment was performed in five replicates.

Evolution experiments

To identify spontaneous mutations increasing AF tolerance, an overnight culture of either 630Δ*erm* or E1 strain was plated on TY containing AF at 5 or 10 µg mL^{-1}. After 4 to 7 days, visible clones were cultured for congelation and MIC experiment. To select and identify adaptive mutations, MIC experiments of either 630Δ*erm* or E1 strain were performed. After 24 h of incubation at 37 °C, the MIC was recorded and the well with bacterial growth visible with the highest AF dose was diluted to perform a new MIC. The experiment was run over 30 days. Samples were frozen every 5 days.

Sequencing

DNA from evolved populations and parental strains were extracted using the NucleoSpin Microbial DNA kit (Macherey-Nagel). Strains were sequenced using Illumina with paired-end 300 bp reads by the dieresis around Plateforme Microbiologie Mutualisée (P2M—Institut Pasteur). The platform provided filtered pair-end reads, de novo assembly and annotation. Identification of SNPs was performed using breseq v0.35.7[86] with default parameters using filtered reads. This software allows to detect mutation relying on read mapping onto the assembled and annotated reference genomes.

Growth curves

After inoculation in an anaerobic cabinet of 96-well plates with a bacterial suspension adjusted to an OD_{600nm} of 0.05, plates were sealed using plate sealers (R&D Systems) and growth curves were assessed by OD_{600nm} measuring every 30 min for 24 h in the GloMax® Explorer system (Promega). The experiment was done in triplicate.

Sporulation assay

The sporulation assay was performed as previously described[39]. Briefly, an overday culture was used to inoculate a 5 mL culture at OD_{600nm} of 0.05. After inoculation, and every 24 h for 4 days, total cells were numerated by serial dilution and spotting on TY + taurocholate 0.05%. Dilutions were then treated with ethanol 96% 1/1 v/v for 1 h to eliminate vegetative cells before new spotting. Percentage of sporulation was calculated by dividing the number of spores by the number of total cells. The experiment was done in five replicates.

Toxin quantification

An overday culture was used to inoculate a fresh culture at an OD_{600nm} of 0.05. After 24 h, the OD_{600nm} was measured and 1 mL of culture was centrifuged. Supernatant was collected and pellet was washed once in PBS before storage at −20 °C. Bacteria were then lysed through an incubation of 40 min at 37 °C in PBS in the presence of DNAse I at 12 µg mL^{-1} (Sigma). Sandwich ELISAs were then performed to quantify free and intracellular toxins A and B in MaxiSorp 96-wells plates (Nunc). For toxin A, PCG4.1 antibody (Biotechne) at 4 µg mL^{-1} was used for capture and LS-C128215 antibody (LS Bio) at 0.1 µg mL^{-1} antibody was used for detection. For toxin B, BM347-N4A8 antibody (BBI Solutions) at 2 µg mL^{-1} was used for capture, while

biotinylated BM347-T4G1 antibody (BBI Solutions) at 1 µg mL^{-1} antibody and streptavidin-HRP (Thermo Scientific) at 125 µg mL^{-1} were used for detection. For revelation, the TMB substrate solution (Thermo Fisher) was used and reaction was stopped with H_2SO_4 at 0.2 M prior quantification through OD_{490nm} measurement. Purified toxin A or B (Sigma) were used for the standard curve that allows toxin quantification. Results were normalized by the OD_{600nm} of the initial culture. The experiment was done in six replicates.

RNA extraction and qRT-PCR

Cultures of the WT strain and the *rsbW*^{STOP} strain were inoculated in TY at OD_{600nm} 0.05 and incubated for 5 h in anaerobiosis. Pellets were resuspended in RNApro solution (MP Biomedicals) and RNA was extracted using the FastRNA Pro Blue Kit (MP Biomedicals). RNA purification was performed using the Direct-zol RNA MiniPrep kit (Zymo Research). cDNAs synthesis and real-time quantitative PCR were performed as previously described[87,88]. In each sample, the quantity of cDNAs of a gene was normalized to the quantity of cDNAs of the *gyrA* gene. The relative change in gene expression was recorded as the ratio of normalized target concentrations (the threshold cycle ΔΔCt method)[89]. Experiment was performed in five biological replicates.

Statistical analysis

For survival on plate, one-way ANOVA was performed followed by Tukey's multiple comparison. For MBC, Mann–Whitney tests were used. To compare MIC distribution between *trxB4* positive and negative strains, a Mann–Whitney test was used. To compare MIC evolution between strain, a two-way ANOVA was performed. For sporulation, multiple *t*-tests were used to compare the rate of sporulation every day. For toxin quantification, unpaired *t*-tests were performed. For LDH assay, unpaired *t*-test was performed. For qPCR, one sample *t*-tests were used with comparison of the fold change to 1. Figures and statistical analysis were performed using the GraphPad Prism (version 10.1.1).

MiPro

Approval for human stool collection was obtained from the local ethics committee (Comité de Protection de Personnes Ile de France IV, IRB00003835 Suivitheque study; registration no. 2012/05NICB). Human stool collection, preparation, storage and MiPro set up were done as previously described[58,60]. Briefly, four healthy male volunteers were recruited for stool sample collection. Approximately 8 g of fresh stools were collected from the volunteers, immediately transferred to anaerobic workstation and then homogenized in 20 mL pre-reduced deoxygenated preservation buffer (10% (v/v) glycerol, 0.1% (w/v) L-cysteine hydrochloride in PBS) in 50 mL sterile conical centrifuge tubes. Prior to usage, the preservation buffer was stored in an anaerobic workstation (5% H_2, 5% CO_2, and 90% N_2) overnight before use. Additional pre-reduced deoxygenated preservation buffer was added make a 20% (w/v) fecal slurry. The mixture was filtered using sterile gauzes to remove large particles, aliquot and stored at −80 °C.

The culture medium was equilibrated in an anaerobic workstation overnight before use. Frozen fecal slurry was thawed at 37 °C with thorough shaking prior to inoculation and diluted at 2% in MiPro medium. AF diluted in DMSO was added at a final concentration of 3, 30 or 300 µg mL^{-1} and DMSO was added as vehicle control at the same volume of AF. Van diluted in DMSO was added at a final concentration of 500 µg mL^{-1}. The plate was covered with vented sterile silicone mats and shaken at 500 rpm at 37 °C for 48 h in the anaerobic workstation. At 24 and 48 h, cultures were centrifuged, and pellets were used for DNA extraction.

16S analysis

Fecal DNA extraction was performed as previously described[90]. Gut microbiota composition and diversity were determined using 16S sequencing. Following PCR, amplicon quality was verified by gel electrophoresis and sent to the @BRIDGe platform for sequencing protocol on an Illumina MiSeq (Illumina, San Diego, CA, USA).

The size of the sequenced pair-end libraries ranged from 33,739 bp to 112,325 bp, representing a total of over 2.6 million 250 bp reads. Reads were processed through Qiime2 (version 2020.8.0)[91]: low-quality reads and sequencing adapters were removed using Cutadapt[92], and sequencing errors were corrected with Dada2[93] using custom parameters (--p-trunc-len-f 230 --p-trunc-len-r 220). Taxonomic assignation of resulted ASVs was done using SILVA trained database (version 138-99)[94] based on scikit-learn's naïve Bayes algorithm[95]. Results were deep analyzed with the Phyloseq package (version 1.34.0)[96] as for the analysis of taxonomic and alpha diversity. Statistical analyses were performed using rstatix (version 0.7)[97] and figures were plotted using the ggplot2 package (version 3.3.5)[98]. Spearman rank correlation analyses were conducted to associate auranofin treatment and microbiota features using the R package rstatix (version 0.7.2). Multivariable association between microbial community abundance and treatment was examined with MaAsLin2[99].

Data availability

The GenBank accession number for the sequences of the evolution experiment is PRJNA1047340. The GenBank accession number for the sequences of the 16S sequencing experiment is PRJNA1083456.

Received: 2 April 2024; Accepted: 20 August 2024;
Published online: 17 September 2024

References

1. Smits, W. K., Lyras, D., Lacy, D. B., Wilcox, M. H. & Kuijper, E. J. Clostridium difficile infection. *Nat. Rev. Dis. Prim.* **2**, 16020 (2016).
2. Schäffler, H. & Breitrück, A. Clostridium difficile—from colonization to infection. *Front. Microbiol.* **9**, 646 (2018).
3. Theriot, C. M. et al. Antibiotic-induced shifts in the mouse gut microbiome and metabolome increase susceptibility to Clostridium difficile infection. *Nat. Commun.* **5**, 3114 (2014).
4. Couturier, J., Davies, K. & Barbut, F. Ribotypes and new virulent strains across Europe. in *Updates on Clostridioides difficile in Europe* (*Advances in Experimental Medicine and Biology*, Vol. 1435) (eds Mastrantonio, P. & Rupnik, M.) 151–168 (Springer International Publishing, 2024).
5. Awad, M. M., Johanesen, P. A., Carter, G. P., Rose, E. & Lyras, D. *Clostridium difficile* virulence factors: insights into an anaerobic spore-forming pathogen. *Gut Microbes* **5**, 579–593 (2014).
6. Aktories, K., Schwan, C. & Jank, T. Clostridium difficile toxin biology. *Annu. Rev. Microbiol.* **71**, 281–307 (2017).
7. Kuehne, S. A. et al. The role of toxin A and toxin B in Clostridium difficile infection. *Nature* **467**, 711–713 (2010).
8. Abt, M. C., McKenney, P. T. & Pamer, E. G. Clostridium difficile colitis: pathogenesis and host defence. *Nat. Rev. Microbiol.* **14**, 609–620 (2016).
9. Naz, F. & Petri, W. A. Host immunity and immunization strategies for Clostridioides difficile infection. *Clin. Microbiol. Rev.* **36**, e00157-22 (2023).
10. Aktories, K., Papatheodorou, P. & Schwan, C. Binary Clostridium difficile toxin (CDT)—a virulence factor disturbing the cytoskeleton. *Anaerobe* **53**, 21–29 (2018).
11. Barbut, F. et al. Clinical features of Clostridium difficile-associated diarrhoea due to binary toxin (actin-specific ADP-ribosyltransferase)-producing strains. *J. Med. Microbiol* **54**, 181–185 (2005).
12. Kelly, C. P. Can we identify patients at high risk of recurrent Clostridium difficile infection? *Clin. Microbiol. Infect.* **18**, 21–27 (2012).
13. Song, J. H. & Kim, Y. S. Recurrent Clostridium difficile infection: risk factors, treatment, and prevention. *Gut Liver* **13**, 16–24 (2019).
14. Meza-Torres, J., Auria, E., Dupuy, B. & Tremblay, Y. D. N. Wolf in sheep's clothing: Clostridioides difficile biofilm as a reservoir for recurrent infections. *Microorganisms* **9**, 1922 (2021).
15. Rubio-Mendoza, D., Martínez-Meléndez, A., Maldonado-Garza, H. J., Córdova-Fletes, C. & Garza-González, E. Review of the impact of

biofilm formation on recurrent Clostridioides difficile infection. *Microorganisms* **11**, 2525 (2023).
16. van Prehn, J. et al. European Society of Clinical Microbiology and Infectious Diseases: 2021 update on the treatment guidance document for Clostridioides difficile infection in adults. *Clin. Microbiol. Infect. Dis.* **27**, S1–S21 (2021).
17. European Centre for Disease prevention and Control. Clostridioides (Clostridium) difficile infections—Annual Epidemiological Report for 2016–2017. https://www.ecdc.europa.eu/en/publications-data/clostridiodes-difficile-infections-annual-epidemiological-report-2016-2017 (2022).
18. Centers for Disease Control and Prevention (U.S.). *Antibiotic Resistance Threats in the United States, 2019* (Centers for Disease Control and Prevention (U.S.), 2019).
19. Di Bella, S. et al. *Clostridioides difficile* infection: history, epidemiology, risk factors, prevention, clinical manifestations, treatment, and future options. *Clin. Microbiol. Rev.* 37, e00135-23 (2024).
20. Chen, J. et al. Cost-effectiveness of bezlotoxumab and fidaxomicin for initial Clostridioides difficile infection. *Clin. Microbiol. Infect. Dis.* **27**, 1448–1454 (2021).
21. Wynn, A. B., Beyer, G., Richards, M. & Ennis, L. A. Procedure, screening, and cost of fecal microbiota transplantation. *Cureus* 15, e35116 (2023).
22. Louie, T. J. et al. Fidaxomicin versus vancomycin for Clostridium difficile infection. *N. Engl. J. Med.* **364**, 422–431 (2011).
23. Minkoff, N. Z. et al. Fecal microbiota transplantation for the treatment of recurrent *Clostridioides difficile* (*Clostridium difficile*). *Cochrane Database Syst. Rev*. **4**, CD013871 (2023).
24. Schwanbeck, J. et al. Characterization of a clinical Clostridioides difficile isolate with markedly reduced fidaxomicin susceptibility and a V1143D mutation in rpoB. *J. Antimicrob. Chemother.* **74**, 6–10 (2019).
25. Marchandin, H. et al. In vivo emergence of a still uncommon resistance to fidaxomicin in the urgent antimicrobial resistance threat Clostridioides difficile. *J. Antimicrob. Chemother.* **78**, 1992–1999 (2023).
26. Wilcox, M. H. et al. Bezlotoxumab for prevention of recurrent Clostridium difficile infection. *N. Engl. J. Med.* **376**, 305–317 (2017).
27. Suarez-Almazor, M. E., Spooner, C., Belseck, E. & Shea, B. Auranofin versus placebo in rheumatoid arthritis. *Cochrane Database Syst. Rev.* **2000**, CD002048 (2000).
28. Harbut, M. B. et al. Auranofin exerts broad-spectrum bactericidal activities by targeting thiol-redox homeostasis. *Proc. Natl. Acad. Sci. USA* **112**, 4453–4458 (2015).
29. AbdelKhalek, A., Abutaleb, N. S., Mohammad, H. & Seleem, M. N. Antibacterial and antivirulence activities of auranofin against Clostridium difficile. *Int. J. Antimicrob. Agents* **53**, 54–62 (2019).
30. Owings, J. P. et al. Auranofin and N-heterocyclic carbene gold-analogs are potent inhibitors of the bacteria Helicobacter pylori. *FEMS Microbiol. Lett.* **363**, fnw148 (2016).
31. Liu, Y. et al. Repurposing of the gold drug auranofin and a review of its derivatives as antibacterial therapeutics. *Drug Discov. Today* **27**, 1961–1973 (2022).
32. Hutton, M. L. et al. Repurposing auranofin as a Clostridioides difficile therapeutic. *J. Antimicrob. Chemother.* **75**, 409–417 (2019).
33. Jackson-Rosario, S. et al. Auranofin disrupts selenium metabolism in Clostridium difficile by forming a stable Au-Se adduct. *J. Biol. Inorg. Chem.* **14**, 507–519 (2009).
34. Abutaleb, N. S. & Seleem, M. N. Auranofin, at clinically achievable dose, protects mice and prevents recurrence from Clostridioides difficile infection. *Sci. Rep.* **10**, 7701 (2020).
35. Abutaleb, N. S. & Seleem, M. N. In vivo efficacy of auranofin in a hamster model of Clostridioides difficile infection. *Sci. Rep.* **11**, 7093 (2021).
36. Ruth, M. M. et al. Auranofin activity exposes thioredoxin reductase as a viable drug target in *Mycobacterium abscessus*. *Antimicrob. Agents Chemother.* **63**, e00449-19 (2019).
37. Elkashif, A. & Seleem, M. N. Investigation of auranofin and gold-containing analogues antibacterial activity against multidrug-resistant Neisseria gonorrhoeae. *Sci. Rep.* **10**, 5602 (2020).
38. AbdelKhalek, A., Abutaleb, N. S., Elmagarmid, K. A. & Seleem, M. N. Repurposing auranofin as an intestinal decolonizing agent for vancomycin-resistant enterococci. *Sci. Rep.* **8**, 8353 (2018).
39. Anjou, C. et al. The multiplicity of thioredoxin systems meets the specific lifestyles of Clostridia. *PLoS Pathog.* **20**, e1012001 (2024).
40. McAllister, K. N., Bouillaut, L., Kahn, J. N., Self, W. T. & Sorg, J. A. Using CRISPR-Cas9-mediated genome editing to generate C. difficile mutants defective in selenoproteins synthesis. *Sci. Rep.* **7**, 14672 (2017).
41. Andreesen, J. R. Glycine metabolism in anaerobes. *Antonie Van. Leeuwenhoek* **66**, 223–237 (1994).
42. Johnstone, M. A. & Self, W. T. d-Proline reductase underlies proline-dependent growth of Clostridioides difficile. *J. Bacteriol.* **0**, e00229-22 (2022).
43. Pavao, A. et al. Reconsidering the in vivo functions of Clostridial Stickland amino acid fermentations. *Anaerobe* **76**, 102600 (2022).
44. Andreesen, J. R. Glycine reductase mechanism. *Curr. Opin. Chem. Biol.* **8**, 454–461 (2004).
45. Buey, R. M. et al. Ferredoxin-linked flavoenzyme defines a family of pyridine nucleotide-independent thioredoxin reductases. *Proc. Natl. Acad. Sci. USA* **115**, 12967–12972 (2018).
46. Doern, C. D. When does 2 plus 2 equal 5? A review of antimicrobial synergy testing. *J. Clin. Microbiol.* **52**, 4124–4128 (2014).
47. Kint, N. et al. The σ^B signalling activation pathway in the enteropathogen *Clostridioides difficile*. *Environ. Microbiol.* **21**, 2852–2870 (2019).
48. Norsigian, C. J. et al. Systems biology analysis of the Clostridioides difficile core-genome contextualizes microenvironmental evolutionary pressures leading to genotypic and phenotypic divergence. *Npj Syst. Biol. Appl.* **6**, 31 (2020).
49. Chandra, H., Sorg, J. A., Hassett, D. J. & Sun, X. Regulatory transcription factors of Clostridioides difficile pathogenesis with a focus on toxin regulation. *Crit. Rev. Microbiol.* **49**, 334–349 (2023).
50. Kint, N. et al. The alternative sigma factor σ^B plays a crucial role in adaptive strategies of *Clostridium difficile* during gut infection: role of σ^B in stress adaptation in *C. difficile*. *Environ. Microbiol.* **19**, 1933–1958 (2017).
51. Soutourina, O. et al. Genome-wide transcription start site mapping and promoter assignments to a sigma factor in the human enteropathogen Clostridioides difficile. *Front. Microbiol.* **11**, 1939 (2020).
52. Cheng, J. K. J. et al. Regulatory role of anti-sigma factor RsbW in Clostridioides difficile stress response, persistence, and infection. *J. Bacteriol.* **205**, e00466-22 (2023).
53. Rizvi, A. et al. Glycine fermentation by C. difficile promotes virulence and spore formation, and is induced by host cathelicidin. *Infect. Immun.* **91**, e00319-23 (2023).
54. Sinha, S. R. et al. Dysbiosis-induced secondary bile acid deficiency promotes intestinal inflammation. *Cell Host Microbe* **27**, 659–670.e5 (2020).
55. Byndloss, M. X. et al. Microbiota-activated PPAR-γ-signaling inhibits dysbiotic Enterobacteriaceae expansion. *Science* **357**, 570–575 (2017).
56. Kint, N. et al. How the anaerobic enteropathogen Clostridioides difficile tolerates low O2 tensions. *mBio* **11**, e01559-20 (2020).
57. Kint, N., Morvan, C. & Martin-Verstraete, I. Oxygen response and tolerance mechanisms in Clostridioides difficile. *Curr. Opin. Microbiol.* **65**, 175–182 (2022).

58. Li, L. et al. An in vitro model maintaining taxon-specific functional activities of the gut microbiome. *Nat. Commun.* **10**, 4146 (2019).
59. Li, L. et al. Berberine and its structural analogs have differing effects on functional profiles of individual gut microbiomes. *Gut Microbes* **11**, 1348–1361 (2020).
60. Zhang, X. et al. Evaluating live microbiota biobanking using an ex vivo microbiome assay and metaproteomics. *Gut Microbes* **14**, 2035658 (2022).
61. Sunwoo, J. et al. Impact of vancomycin-induced changes in the intestinal microbiota on the pharmacokinetics of simvastatin. *Clin. Transl. Sci.* **13**, 752–760 (2020).
62. Dubois, T. et al. A microbiota-generated bile salt induces biofilm formation in Clostridium difficile. *NPJ Biofilms Microbiomes* **5**, 14 (2019).
63. Gonzales, M. et al. Faecal pharmacokinetics of orally administered vancomycin in patients with suspected Clostridium difficile infection. *BMC Infect. Dis.* **10**, 363 (2010).
64. Capparelli, E. V., Bricker-Ford, R., Rogers, M. J., McKerrow, J. H. & Reed, S. L. Phase I clinical trial results of auranofin, a novel antiparasitic agent. *Antimicrob. Agents Chemother.* **61** https://doi.org/10.1128/aac.01947-16 (2016).
65. Cole, J. A. Anaerobic bacterial response to nitrosative stress. *Adv. Microb. Physiol*. **72**, 193–237 (2018).
66. Poole, L. B. The basics of thiols and cysteines in redox biology and chemistry. *Free Radic. Biol. Med.* **80**, 148–157 (2015).
67. Marreddy, R. K. R., Olaitan, A. O., May, J. N., Dong, M. & Hurdle J. G. Ebselen not only inhibits Clostridioides difficile toxins but displays redox-associated cellular killing. *Microbiol. Spectr.* **9**, e00448-21 (2021).
68. Lu, J. et al. Inhibition of bacterial thioredoxin reductase: an antibiotic mechanism targeting bacteria lacking glutathione. *FASEB J.* **27**, 1394–1403 (2013).
69. McAllister, K. N., Martinez Aguirre, A. & Sorg, J. A. The selenophosphate synthetase gene, selD, is important for Clostridioides difficile physiology. *J. Bacteriol.* **203**, e00008-21 (2021).
70. Johnstone, M. A., Holman, M. A. & Self, W. T. Inhibition of selenoprotein synthesis is not the mechanism by which auranofin inhibits growth of Clostridioides difficile. *Sci. Rep.* **13**, 14733 (2023).
71. Chen, H., Liu, Y., Liu, Z. & Li, J. Mutation in trxB leads to auranofin resistance in Staphylococcus aureus. *J. Glob. Antimicrob. Resist.* **22**, 135–136 (2020).
72. Uziel, O., Borovok, I., Schreiber, R., Cohen, G. & Aharonowitz, Y. Transcriptional regulation of the Staphylococcus aureus thioredoxin and thioredoxin reductase genes in response to oxygen and disulfide stress. *J. Bacteriol.* **186**, 326–334 (2004).
73. Stogios, P. J. & Savchenko, A. Molecular mechanisms of vancomycin resistance. *Protein Sci.* **29**, 654–669 (2020).
74. Taib, N. et al. Genome-wide analysis of the Firmicutes illuminates the diderm/monoderm transition. *Nat. Ecol. Evol.* **4**, 1661–1672 (2020).
75. Maus, I. et al. The role of petrimonas mucosa ING2-E5AT in mesophilic biogas reactor systems as deduced from multiomics analyses. *Microorganisms* **8**, 2024 (2020).
76. Maier, L. et al. Extensive impact of non-antibiotic drugs on human gut bacteria. *Nature* **555**, 623–628 (2018).
77. Rocha, E. R., Tzianabos, A. O. & Smith, C. J. Thioredoxin reductase is essential for thiol/disulfide redox control and oxidative stress survival of the anaerobe bacteroides fragilis. *J. Bacteriol.* **189**, 8015–8023 (2007).
78. Szczepanowski, P. et al. HP1021 is a redox switch protein identified in Helicobacter pylori. *Nucleic Acids Res.* **49**, 6863–6879 (2021).
79. Newton, G. L. et al. Distribution of thiols in microorganisms: mycothiol is a major thiol in most actinomycetes. *J. Bacteriol.* **178**, 1990–1995 (1996).
80. Ogata, F. T., Branco, V., Vale, F. F. & Coppo, L. Glutaredoxin: discovery, redox defense and much more. *Redox Biol.* **43**, 101975 (2021).
81. Holmgren, A. Hydrogen donor system for Escherichia coli ribonucleoside-diphosphate reductase dependent upon glutathione. *Proc. Natl. Acad. Sci. USA* **73**, 2275–2279 (1976).
82. Aslund, F., Ehn, B., Miranda-Vizuete, A., Pueyo, C. & Holmgren, A. Two additional glutaredoxins exist in Escherichia coli: glutaredoxin 3 is a hydrogen donor for ribonucleotide reductase in a thioredoxin/glutaredoxin 1 double mutant. *Proc. Natl. Acad. Sci. USA* **91**, 9813–9817 (1994).
83. Meyer, Y., Buchanan, B. B., Vignols, F. & Reichheld, J. P. Thioredoxins and glutaredoxins: unifying elements in redox biology. *Annu. Rev. Genet.* **43**, 335–367 (2009).
84. Feng, X. et al. Synergistic activity of colistin combined with auranofin against colistin-resistant gram-negative bacteria. *Front. Microbiol*. **12**, 676414 (2021).
85. Wensel, C. R., Pluznick, J. L., Salzberg, S. L. & Sears, C. L. Next-generation sequencing: insights to advance clinical investigations of the microbiome. *J. Clin. Invest.* **132**, e154944 (2022).
86. Deatherage, D. E. & Barrick, J. E. Identification of mutations in laboratory evolved microbes from next-generation sequencing data using breseq. *Methods Mol. Biol.* **1151**, 165–188 (2014).
87. Saujet, L., Monot, M., Dupuy, B., Soutourina, O. & Martin-Verstraete, I. The key sigma factor of transition phase, SigH, controls sporulation, metabolism, and virulence factor expression in Clostridium difficile▽. *J. Bacteriol.* **193**, 3186–3196 (2011).
88. Soutourina, O. A. et al. Genome-wide identification of regulatory RNAs in the human pathogen Clostridium difficile. *PLoS Genet.* **9**, e1003493 (2013).
89. Livak, K. J. & Schmittgen, T. D. Analysis of relative gene expression data using real-time quantitative PCR and the $2-\Delta\Delta CT$ method. *Methods* **25**, 402–408 (2001).
90. Lamas, B. et al. CARD9 impacts colitis by altering gut microbiota metabolism of tryptophan into aryl hydrocarbon receptor ligands. *Nat. Med.* **22**, 598–605 (2016).
91. Bolyen, E. et al. Reproducible, interactive, scalable and extensible microbiome data science using QIIME 2. *Nat. Biotechnol.* **37**, 852–857 (2019).
92. Martin, M. Cutadapt removes adapter sequences from high-throughput sequencing reads. *EMBnet J.* **17**, 10–12 (2011).
93. Callahan, B. J. et al. DADA2: high resolution sample inference from Illumina amplicon data. *Nat. Methods* **13**, 581–583 (2016).
94. Quast, C. et al. The SILVA ribosomal RNA gene database project: improved data processing and web-based tools. *Nucleic Acids Res.* **41**, D590–D596 (2013).
95. Pedregosa, F. et al. Scikit-learn: Machine Learning in Python. *J. Mach. Learn. Res*. **12**, 2825–2830 (2011).
96. McMurdie, P. J. & Holmes, S. phyloseq: an R package for reproducible interactive analysis and graphics of microbiome census data. *PLoS ONE* **8**, e61217 (2013).
97. Kassambara, A. rstatix: pipe-friendly framework for basic statistical tests. https://cran.r-project.org/web/packages/rstatix/index.html (2023).
98. Wickham, H. et al. *ggplot2: Elegant Graphics for Data Analysis*. Springer-Verlag New York. https://ggplot2.tidyverse.org (2016).
99. Mallick, H. et al. Multivariable association discovery in population-scale meta-omics studies. *PLoS Comput. Biol.* **17**, e1009442 (2021).
100. European Committee on Antimicrobial Susceptibility Testing. eucast: Clinical breakpoints and dosing of antibiotics. https://www.eucast.org/clinical_breakpoints.

Acknowledgements

This work was supported by the Fondation pour la Recherche Médicale (grant numbers ECO202006011710 and FDT202304016494) and by the Institut Pasteur for the funding of the PhD contract of C.A. and by the Institut Universitaire de France for I.M.-V. The funders played no role in study design, data collection, analysis and interpretation of data, or the writing of this manuscript. We thank Laure Diancourt for her help with the sequencing of the strains, Elena Capuzzo for her experimental help, Marie-Noelle Rossignol and Kassandra Alexis-Alphonse

(Plateforme @BRIDGe, INRAe) for 16S sequencing, and Harry Sokol for helpful discussions.

Author contributions

I.M.V. and C.A. designed the research. I.M.V. and C.M. supervised experimental work and I.M.V., C.A., M.R., E.B. and L.C. performed the experiments. N.R., I.A.S. and M.B. performed the MiPro experiment and the 16S analysis. J.L. analyzed the WGS of evolved strains. B.D. and F.B. provided material. I.M.V. and C.A. wrote the manuscript, and all authors reviewed it. All authors have read and approved the manuscript.

Competing interests

The authors declare no competing interests.

Additional information

Supplementary information The online version contains supplementary material available at https://doi.org/10.1038/s41522-024-00551-3.

Correspondence and requests for materials should be addressed to Isabelle Martin-Verstraete.